ELSEVIER

Catalysis Today 49 (1999) 79–86

CATALYSIS TODAY

Transformations of ferrihydrite during calcination and sulphidation

Klaus Hellgardt*, David Chadwick

Department of Chemical Engineering and Chemical Technology, Imperial College of Science, Technology and Medicine, Prince Consort Road, London SW7 2BY, UK

Abstract

The chemical and morphological transformation of ferrihydrite during calcination and subsequent sulphidation is addressed using in situ techniques (BET, XPS, TPS). The sulphidation process (in 10% H_2S/H_2) appears to be diffusion controlled. Surface and bulk composition after sulphidation are in close agreement ($FeS_{1.4}$ – pyrrhotite) and suggest the presence of excess sulphur. This excess sulphur can be removed via simple hydrogenation to yield FeS (troilite). Strong structural collapse occurs during sulphidation and is caused by agglomeration/sintering of primary crystallites. The BET surface area of the sulphided material is found to be very low (2 m^2/g).

Keywords: Ferrihydrite; Hematite; Pyrrhotite; Troilite; Precipitation; Sulphidation; BET; XPS; TPS

1. Introduction

Modified iron catalysts are widely used as catalysts for ammonia synthesis, Fischer–Tropsch synthesis, styrene production from ethylbenzene and high temperature shift reactions, e.g. [1–4]. They are further applied as high temperature sorbents for H_2S scrubbing [5]. Iron based catalysts have also been suggested for the hydrotreatment of extra heavy fuels where the catalyst is discarded with the residue [6–8]. These catalysts have the advantage of being cheap and environmentally safe. Their catalytic activity, compared to other, conventional hydrotreating catalysts such as supported CoMo or NiMo is relatively low [9]. In this context it is important to understand the transformation of the precursor (usually iron oxyhydroxide via precipitation from inorganic salt solution) during the calcination and subsequent sulphidation process, yielding the active catalyst, a substoichiometric iron sulphide $Fe_{(1-x)}S$. These transformations are addressed in this paper using in situ techniques.

2. Experimental

Ferrihydrite was precipitated from nitrate solution at a pH of 7.0 using a *continuous* precipitation apparatus. Details of the apparatus and the precipitation procedure are given elsewhere [10]. Quasi in situ techniques (BET, XPS) which have been developed at Imperial College for the characterisation of oxidic and the sulphided materials were employed in the characterisation of the different materials. These techniques have been described elsewhere [11,12].

---

*Corresponding author. Present address: Department of Chemical Engineering, Loughborough University, Loughborough, Leicestershire LE11 3TU, UK.

PII: S0920-5861(98)00411-8

Temperature programmed reduction and sulphidation experiments were carried out up to 1000°C in pure H_2 and 10% H_2S/H_2 atmospheres, respectively, using purpose built reactor systems [13,14]. Approximately 500 mg of catalysts was charged. The gas flow rate was set at 200 ml/min (STP) and a heating rate of 10°C/min was applied. XRD data were obtained with a Philips PW1710 automated powder diffractometer. Cu K_α radiation (0.15405 nm) was applied at 40 kV and 50 mA using a monochromator. The 2θ angle was varied from 0 to up to 120° in steps of 0.02. Small powdered samples were usually distributed onto an Si ⟨1 1 1⟩ wafer using acetone to evenly spread the small particles.

3. Results and discussion

3.1. XRD and BET

Iron catalysts were prepared by varying the pH of precipitation in order to establish the pH sensitivity of the morphological properties of the catalysts. The BET surface areas of all catalysts were found to be rather high at around 140–180 m^2/g. No particular trend of the BET surface areas as a function of the pH of precipitation could be detected. The average pore size was also rather constant at about 5 nm suggesting interparticular spaces [15]. The pure ferrihydrite precipitated at pH 7.0 was chosen for further investigation. Fig. 1 shows the XRD patterns obtained for the dried, calcined and subsequently sulphided pure ferrihydrite catalyst. The diffraction pattern for the dried sample (120°C, 4 h) corresponds to 2-line ferrihydrite [15]. The pattern of the calcined sample (400°C, 12 h) can be attributed to hematite or Fe_2O_3. The diffraction pattern after sulphidation (10 vol% H_2S/H_2 at 400°C, 1 h) corresponds to troilite or FeS. Clearly, the crystallinity of the dried ferrihydrite is low and is much increased for the calcined and the sulphided sample. Using our quasi in situ BET technique, average pore sizes and BET surface areas of the dried, calcined and sulphided iron catalyst were determined, Fig. 2. It is evident from Fig. 2 that strong structural collapse occurs during the calcination and particularly during the sulphidation process. The BET surface area of the sulphided catalyst (troilite) is found to be significantly lower (2 m^2/g) than that of the precursor (ferrihydrite, 180 m^2/g). The average pore size on the other hand is increased from 5 nm (ferrihydrite) to over 35 nm (troilite). Particle sizes determined from the line widths of the diffraction peaks (using the Scherrer equation, e.g. [16]) suggest an average particle size for the calcined sample of approximately 16.8 nm perpendicular to the ⟨3 0 0⟩ plane. A particle size of 13 nm was determined for the sulphided sample (⟨1 1 4⟩ plane). Using the BET surface areas and quoted densities [17], particle sizes can also be estimated by simple geometrical considerations. This leads to an approximate particle size for the ferrihydrite of 9 nm. The particle size for the hematite would be about 40 nm. In the case of the troilite 630 nm may be estimated. The latter two values do not correspond very well to those determined from

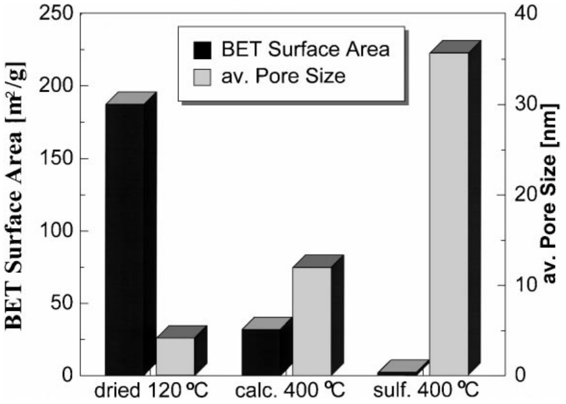

Fig. 2. BET surface areas and average pore sizes after different treatments of Fe pH 7.0.

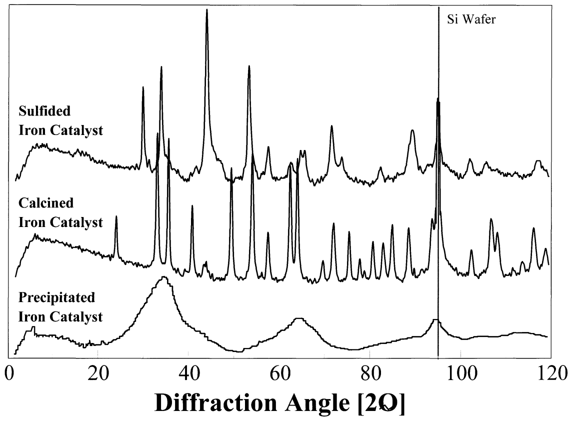

Fig. 1. XRD patterns of dried, calcined and sulphided iron catalyst.

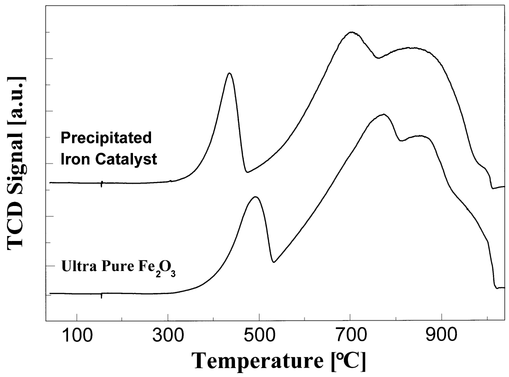

Fig. 3. TPR of iron catalysts.

the XRD data. However, sintering, twinning and/or agglomeration of small primary crystallites would explain the discrepancy between those values.

3.2. TPR, TPS and TPR-S

Temperature programmed reduction was carried out on the calcined, precipitated iron catalyst (hematite) and for comparison on an ultra pure iron oxide (99.999 wt%) obtained from Aldrich Chemicals to probe the reduction behaviour of the precipitated iron catalyst. The TPR spectra of the ultra pure Fe_2O_3 and that of the calcined, precipitated iron catalyst (pH 7.0) are given in Fig. 3. Three similar peaks were recorded for both samples, which may be assigned to the following reduction sequence of iron oxide [18–20]:

$$\text{I}: \ 3Fe_2O_3 + H_2 \underset{(\alpha\text{-reduction})}{\longrightarrow} 2Fe_3O_4 + H_2O$$

$$\text{II}: \ 2Fe_3O_4 + 2H_2 \underset{(\beta\text{-reduction})}{\longrightarrow} 6FeO + 2H_2O$$

$$\text{III}: \ 6FeO + 6H_2 \underset{(\chi\text{-reduction})}{\longrightarrow} 6Fe + 6H_2O$$

Iron oxide (hematite) reduces around 400°C to magnetite Fe_3O_4 which is further reduced to FeO (wüstite) from 550°C and subsequently to metallic Fe at around 1000°C. Reduction is not complete for both samples, the ultra pure Fe_2O_3 being reduced by 89.89% and the precipitated iron catalyst by 83.14%, respectively. The first peak in the spectra, corresponding to the partial reduction of Fe_2O_3 to Fe_3O_4 comprises of approximately 7.58% reduction in the case of the ultra pure Fe_2O_3 and 8.36% reduction of the precipitated iron catalyst. This corresponds roughly to the theoretical value (11%) which can be obtained from the stoichiometry of the reaction. It is this partial reduction which is important in the evaluation of iron catalysts for hydrotreating processes as the relevant temperature scale to be considered in hydrotreating reactions lying in the range up to 450°C. The spectrum of the ultra pure Fe_2O_3 is shifted towards higher reduction temperatures as compared to the spectrum of the precipitated catalyst. This is probably due to the different particle sizes of the two samples. The ultra pure Fe_2O_3 exhibited a BET surface area of approximately 2.6 m^2/g while the calcined, precipitated iron catalyst had a BET surface area of some 30 m^2/g. The average particle size of the precipitated catalyst is hence about 10 times smaller than that of the ultra pure Fe_2O_3. Particle size strongly affects the rate of diffusion of hydrogen during the reduction process and hence causes the apparent delay in the case of the ultra pure material. The same argument applies for the comparably more pronounced α-reduction of the precipitated iron catalyst. The lower degree of reduction achieved for the precipitated catalyst may be due to some nitrate retention even after calcination. Temperature programmed sulphiding and reduction of the sulphide was carried out on the precipitated iron catalyst (pH 7.0, calcined at 400°C for 12 h). Fig. 4 shows the TPS spectra or patterns recorded with a TCD detector (H_2) and a UV detector (H_2S) as a function of the catalyst temperature. The isothermal H_2S uptake of the catalyst was determined as 6×10^{-2} mol H_2S/mol Fe. A much higher H_2S uptake was observed by Baird et al. [21] for pellets of

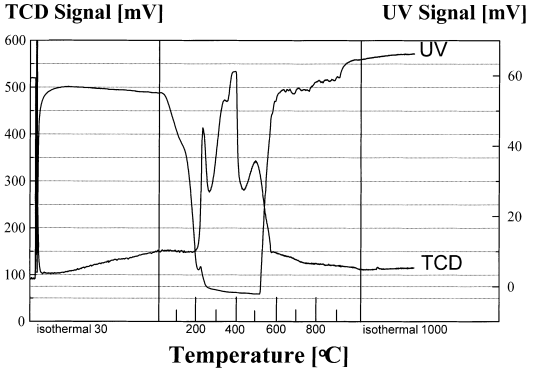

Fig. 4. TPS of precipitated iron catalyst.

feroxyhyte. This can be attributed to the large surface area (180 m^2/g) of their material which had not been calcined prior to the H_2S exposure. The sulphidation of our catalyst starts essentially at room temperature and is complete (no further H_2S uptake recorded) at approximately 550°C. A similar temperature is quoted by Andres et al. [22]. Two features can be observed at the low temperature side of the H_2S uptake: a shoulder at around 100°C and a small peak at 240°C. The corresponding H_2 pattern (H_2 consumption during sulphiding) is more complicated: the envelope shows four peaks at 240°C, 350°C, 400°C and 510°C, respectively. The initial H_2S uptake is not accompanied by any hydrogen consumption or release which suggests that at low temperatures either OH–SH exchange occurs, or that the H_2S adsorbs on coordinatively unsaturated sites (CUS), replacing the adsorbed water. Then, from 200°C onwards H_2 is consumed during H_2S uptake. The apparent peak at 240°C may be artificial and could have been caused by H_2 production around 260°C (valley in the H_2 pattern). H_2 production in this temperature region might result from the decomposition of surface SH groups or from the formation of excess sulphur (S_x) [23,24].

The major peak of the H_2 pattern coincides with the reduction temperature of bulk Fe_2O_3 (Fe^{3+}) to Fe_3O_4 (see TPR). Subsequent sulphidation of the oxygen deficient magnetite to e.g. $Fe_{(1-x)}S$ or Fe_2S_3 occurs [18,21,23,24]. Initial reduction and subsequent sulphidation is quite likely as the diffusion of hydrogen into the bulk of the material proceeds much faster than the diffusion of H_2S, leading to a core of partly reduced iron oxide with a sulphide layer [25]. The total H_2 consumption amounts to 0.156 mol H_2/mol Fe which would mean that if all hydrogen was consumed for iron oxide reduction, approximately 93.3% of the initial Fe_2O_3 would have been reduced to Fe_3O_4. An explanation for the H_2 consumption peak at 510°C may be that the actual sulphidation is complete around 400°C and that some of the formed sulphide species reduce at higher temperatures, resulting in an H_2S release which is overlapped by further consumption at other sites, hence remains undetected. The overall H_2S consumption (including the isothermal uptake) during the TPS experiment was determined as 1.4 mol H_2S/mol Fe. This immediately translates to a bulk stoichiometry of $FeS_{1.4}$ corresponding to a sulphur rich form of pyrrhotite ($Fe_{(1-x)}S$) or indeed Fe_2S_3.

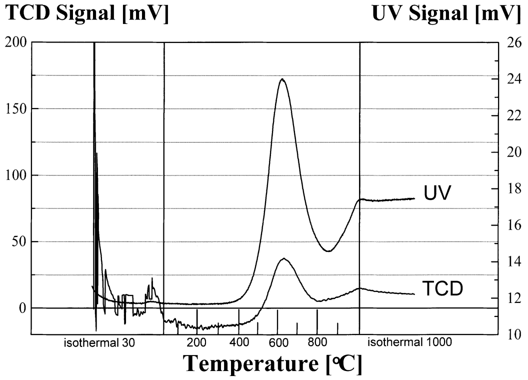

Fig. 5. TPR-S of precipitated iron catalyst.

After sulphidation up to 1000°C the catalyst was reduced in H_2/Ar, Fig. 5 (TPR-S). The H_2S and H_2 signal show a similar pattern. Both detectors recorded a major peak (H_2S release and simultaneous H_2 consumption) at 630°C. The hydrogen consumption corresponds to only about one-half of the H_2S released. From the amount of H_2S released during the reduction of the pyrrhotite (0.3 mol H_2S/mol Fe) a stoichiometry of $FeS_{1.1}$ would follow. But clearly, the reduction process is not complete as can be deduced from Fig. 5. Since the previous TPS experiment was carried out up to 1000°C, a very stable form of iron sulphide may have been produced (pyrite-like structure).

3.3. *Quasi in situ XPS*

Quasi in situ XPS was performed on the precipitated iron oxide to establish the surface composition after the sulphiding and the subsequent reduction process. The experimental details of the treatment conditions are given in Table 1. Fig. 6 shows the

Table 1
Treatment sequence and conditions for precipitated ferrihydrite

Treatment	Notation	Gas	Conditions
1	Sulphided I	10% H_2S/H_2	400°C/1 h
2	Reduced	100% H_2	400°C/1 h
3	Sulphided II	10% H_2S/H_2	400°C/1 h
4	Nitrogen	100% N_2	400°C/1 h
5	Sulphided III	10% H_2S/H_2	400°C/1 h

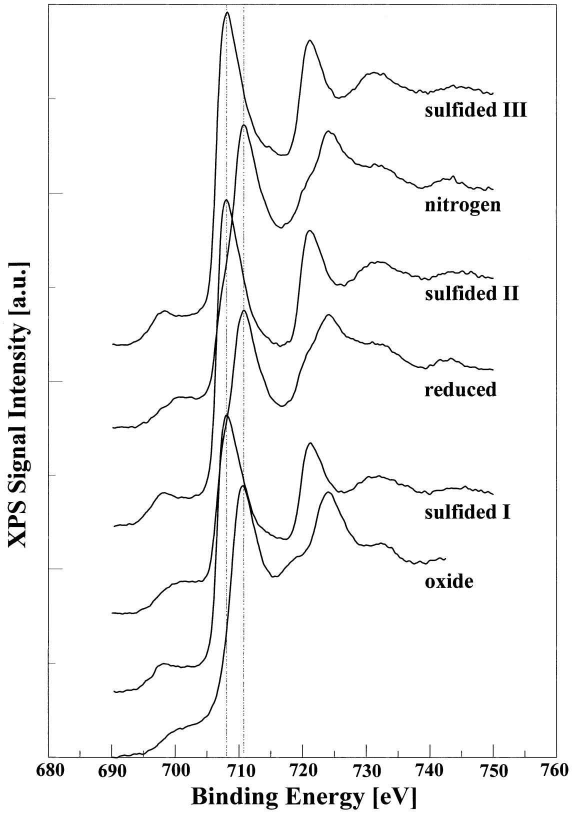

Fig. 6. Fe_2p spectra of ultra pure Fe_2O_3.

Table 2
Binding energies of major peak envelopes after various treatments

Treatment	Binding Energy (eV)		
	$Fe2p_{3/2}$	S2p	O1s
Oxide	710.4	–	529.7
Sulphided I	707.8	161.6	532.6
Reduced	710.4	161.3	530.0
Sulphide II	707.6	161.5	532.5
Nitrogen	710.5	161.2	530.0
Sulphide III	707.7	161.3	532.5

BE corrected for C1s=284.6 eV.

Table 3
Estimated atomic ratios after various treatments

Treatment	Estimated atomic ratio[a]		
	$S2p/Fe_2p$	O1s/Fe2p	Surface stoichiometry
Oxide	–	1.58	$FeO_{1.58}$
Sulphided I	1.41	0.09	$FeS_{1.41}O_{0.09}$
Reduced	0.40	1.29	$FeS_{0.40}O_{1.29}$
Sulphide II	1.46	0.30	$FeS_{1.46}O_{0.3}$
Nitrogen	0.47	1.25	$FeS_{0.47}O_{1.25}$
Sulphide III	1.48	0.26	$FeS_{1.48}O_{0.26}$

[a] Sensitivity factors from Wagner et al. [26].

spectra of the Fe2p transition collected after treatment of the sample as described in Table 1 and also denoted next to the spectrum. Table 2 lists the determined binding energies (BE) of the major peak envelope of the $Fe2p_{3/2}$-transition, the S2p- and the O1s-transition, as referenced to C1s at 284.6 eV. Table 3 shows the estimated atomic S/Fe and O/Fe ratios as well as the resulting stoichiometry, using sensitivity factors published by Wagner et al. [26].

The BE determined for the initial oxidic material was 710.4 eV which is lower than the reported value of 711.0 eV for Fe^{3+} in Fe_2O_3 [27,28]. Sulphidation yielded iron sulphide with a surface atomic sulphur/metal ratio of 1.41 commonly referred to as $Fe_{(1-x)}S$ (pyrrhotite) [29]. Small amounts of surface oxygen were still detectable (O/Fe=0.09). Upon reduction the $Fe2p_{3/2}$ BE increased to the initial value of the oxide (710.4 eV) with a shoulder at the lower BE side. About 71% of the surface sulphur was replaced by oxygen, the oxygen/metal ratio being 1.29. This is probably caused by diffusion of oxygen from the underlying Fe_2O_3. Resulphidation re-established the sulphided state of the sample with an $Fe2p_{3/2}$ BE of 707.6 eV. The sulphur/metal ratio was determined to be 1.46, similar to the first sulphidation. A larger quantity of oxygen remained on the surface, O/Fe=0.3. To evaluate, if the re-occurrence of the surface oxide is only a function of the H_2S partial pressure or if a reducing atmosphere is required, the sample was subsequently treated with 100% N_2 at 400°C. This caused the $Fe2p_{3/2}$ BE to increase again to the value of the oxide (710.5 eV). Again some 67% of the surface sulphur was removed. Another sulphidation cycle yielded the well established $Fe2p_{3/2}$ BE of 707.7 eV and a sulphur/metal ratio of 1.48. The S2p BE in the case of the sulphided samples exhibits values around 161.5 eV which are slightly higher than the value expected for S^{2-} in the pyrrhotite structure (161.2 eV) [29]. This may be explained by the relatively high sulphur/metal ratios observed. The state of this excess sulphur is not clear though. Jones et al. [29]

suggest, based on the modelling of XRD data, the existence of linear chains of S_n polysulphide like structures giving rise to the shifted BE. The formation of sulphate species which would contribute to a higher S2p BE was not observed. Even when the catalyst reverted to the oxidic state (containing still considerable amounts of surface sulphur) the sulphur and the oxygen on the surface did not combine to form sulphate species, although the O1s BE was strongly affected by the changing surface composition (shift of about 2.5 eV). This may be explained by the formation of an oxysulphide or the presence of large amounts of hydroxyl groups on the surface of the catalyst after the sulphiding treatment. The atomic surface sulphur/metal ratio of 1.4 is exactly the same as the bulk stoichiometry determined in the TPS experiment discussed in the previous paragraph. This is clear evidence that the surface composition in our experiment is in thermodynamic equilibrium with the bulk. As pointed out before, the re-occurrence of surface oxidic material may be caused by oxygen diffusion from the underlying bulk iron oxide. This is only possible, if a surface sulphide skin is formed which does not allow the sulphidation process to progress deeper into the bulk of the sample. Compacted sample discs can also restrict H_2S access. This leaves a large reservoir of oxygen in the bulk which may move to the surface via interdiffusion in a reducing or even low H_2S level atmosphere. The experiment carried out under pure nitrogen atmosphere is clear proof that the H_2S concentration is the parameter which leads to the surface composition oscillation. This is in very good agreement with thermodynamic data [30] which suggest that Fe_3O_4 is more stable than FeS in an atmosphere containing less than 250–300 ppm H_2S. This is an H_2S level which can easily be achieved in the quasi in situ reaction cell of our ESCA III if no H_2S is introduced into the reactor gas stream. Levels below 50 ppm have been measured there, resulting from H_2S desorption from the stainless steel walls. For comparison reasons quasi in situ XPS was carried out on a model system (Fe_2O_3 supported on an Si wafer) and on a slab of natural pyrite (FeS_2). The model system was examined to establish the surface composition after sulphidation independent of diffusion restrictions. The pyrite was analysed as it forms the sulphur richest iron sulphide species. Both samples were reduced at 400°C with pure H_2 to investigate the stability of the sulphide under reducing conditions. Table 4 gives the BE and estimated atomic sulphur/iron ratios of the Si supported iron catalyst after sulphidation and reduction.

Table 4
Binding energies and estimated atomic ratios for Fe_2O_3 supported on Si wafer

Treatment	Binding energy $Fe2p_{3/2}$ (eV)	Binding energy S2p (eV)	Atomic ratio[a] S2p/$Fe2p_{3/2}$
Oxide	710.6	–	–
Sulphided	707.4	161.4	1.74
Reduced	707.7	161.2	1.06

BE corrected for C1s=284.6 eV.
[a] Sensitivity factors from Wagner et al. [26].

A slightly different picture emerges from the sulphiding and reduction experiments carried out on the model catalyst (Fe/Si wafer). The $Fe2p_{3/2}$ BE is now closer to the value for Fe^{3+} in hematite (711.0 eV). After sulphidation the $Fe2p_{3/2}$ BE decreases to 707.4 eV which corresponds to pyrrhotite [29]. A rather high sulphur/metal ratio was established which can again be explained by a sulphur enriched form of pyrrhotite as no sulphate species could be detected. The S2p BE which is higher than expected for the S^{2-} in pyrrhotite may be a support to this view. Groot et al. [31] claim, based on Mössbauer experiments, that residual nitrate may be responsible for elemental sulphur deposition which in turn causes the higher S2p BE. Neither elemental sulphur nor residual nitrate could be detected on the present model catalyst. Upon reduction the $Fe2p_{3/2}$ BE increased slightly to 707.7 eV and the S/Fe ratio decreased to 1.06 which now corresponds to FeS (troilite). This ratio was also found by Groot et al. [31] for the highest Fe/C loadings of their catalysts. Thermodynamic calculations for FeS indicate that this sulphide is stable under reducing conditions down to a background H_2S level of 20 ppm. This low H_2S concentration cannot be achieved in our quasi in situ gas cell due to continuous H_2S desorption from the reactor walls in the order of 50 ppm. A comparison with the in situ experiments carried out on the bulk Fe_2O_3 shows that the transformation of both catalysts into pyrrhotite/troilite during sulphidation proceeds at a rather similar manner. The reduction behaviour of the Si supported sulphide is different due to the oxygen diffusion effect in the case of the bulk catalyst. The estimated atomic ratios and BE of the

Table 5
Binding energies and estimated atomic ratios of natural pyrite

Treatment	Binding energies (eV)			Atomic ratios[a]	
	$Fe2p_{3/2}$	S2p	O1s	$S2p/Fe2p_{3/2}$	$O1s/Fe2p_{3/2}$
Untreated	706.0	161.7	531.6	2.46	1.21
Reduced	706.4	161.9	531.9	2.08	0.86

BE corrected for C1s=284.6 eV.
[a] Sensitivity factors from Wagner et al. [26].

untreated and reduced natural pyrite are given in Table 5. The $Fe2p_{3/2}$ BE of the untreated pyrite was rather low with 706.0 eV compared to literature values of 706.5 eV [29,32,33]. Strong surface enrichment with sulphur and oxygen was observed, leading to high atomic ratios. This is supported by the high BE of the O1s and the S2p transitions. Reduction of the pyrite slab removed some of the surface sulphur and oxygen. The $Fe2p_{3/2}$ BE is now in good agreement with published data. The estimated sulphur/metal ratio of 2 corresponds very well with the stoichiometry of FeS_2. It is clear that a natural crystal always contains a considerable amount of oxygen in the lattice [33], hence the amount of surface oxygen present. An explanation for the high BE of the O1s and the S2p transition is not apparent other than the one put forward in the previous section, that these values are due to some oxysulphide or hydroxyl groups present.

4. Conclusions

Strong surface area collapse occurs during calcination and particularly during sulphidation of precipitated ferrihydrite. The collapse appears to be caused by agglomeration processes. The sulphidation of the material proceeds via reduction and subsequent oxygen/sulphur exchange (sulphidation) and is diffusion controlled. Bulk and surface composition are in close agreement exhibiting a stoichiometry of $FeS_{1.4}$ (sulphur rich pyrrhotite). The excess sulphur S_x is not present as sulphate and can be removed via hydrogenation, yielding FeS (troilite).

Acknowledgements

We would like to thank Prof. J. Moulijn, Dr. A.D. van Langeveld and Dr. J.P. Janssens for the opportunity to use their dedicated TPS system at Delft University and also for their valuable assistance during the analysis of the acquired data.

We would also like to acknowledge the financial support of this project by the European Union and the British Council.

References

[1] G.A. Somorjai, Introduction to Surface Chemistry and Catalysis, Wiley, New York, 1994.
[2] B. Fastrup, M. Muhler, H.N. Nielsen, L.P. Nielsen, J. Catal. 69 (1993) 135.
[3] H.H. Kung, M.C. Kung, B.L. Yang, J. Catal. 69 (1981) 506.
[4] D.P. Hoffmann, M. Houalla, A. Proctor, D.M. Hercules, Appl. Spectrosc. 46(3) (1992) 489.
[5] S.S. Tamhankar, M. Hasatani, C.Y. Wen, Chem. Eng. Sci. 36 (1981) 1181.
[6] I.E. Maxwell, J.E. Naber, K.P. de Jong, Appl. Catal. A 113 (1994) 153.
[7] K. Niemann, VEBA OEL AG, Tagungsbericht 9001, DGMK-Haupttagung (1990) 239.
[8] H. Charcosset, A. Genard, in: I. Romley (Ed.), Graham and Trotman, 1987, p. 339.
[9] B. Delmon, Catal. Lett. 22 (1993) 1.
[10] K. Hellgardt, D. Chadwick, Proceedings of IChemE Research Event, vol. 1, London, 1994, p. 595.
[11] A. Oen, K. Hellgardt, D. Chadwick, Bull. Soc. Chim. Belg. 104(4)(5) (1995) 317.
[12] K. Hellgardt, D. Chadwick, Proceedings of the First European Congress on Chemical Engineering, Florence, vol. 3, 1997, p. 2279.
[13] D. Chadwick, P.J.R. O'Malley, J. Chem. Soc., Faraday Trans. I 83(P7) (1987) 2227.
[14] P. Arnoldy, J.L. DeBooys, B. Scheffer, J.A. Moulijn, J. Catal. 961 (1985) 122.
[15] U. Schwertmann, R.M. Cornell, in: Iron Oxides in the Laboratory, VCH, Weinheim, 1991.
[16] H.P. Klug, L.E. Alexander, in: X-Ray Diffraction Procedures, Wiley, New York, 1974.
[17] R.C. Weast (Ed.), CRC Handbook of Chemistry and Physics, 67th ed., CRC Press, Boca Raton, FL, 1987.
[18] V. Patrick, G.R. Gavalas, Ind. Eng. Chem. Res. 32 (1993) 519.
[19] X. Gao, J. Shen, Y. Hsia, Y. Chen, J. Chem. Soc., Faraday Trans. 89(7) (1993) 1079.
[20] J.-F. Lee, W.-S. Chern, M.-D. Lee, Can. J. Chem. Eng. 70 (1992) 511.
[21] T. Baird, K.C. Campbell, P.J. Holliman, R. Hoyle, D. Stirling, B.P. Williams, J. Chem. Soc., Faraday Trans. 92(3) (1996) 445.
[22] M. Andres, H. Charcosset, L. Davignon, G. Djega-Mariadassou, J.-P. Joly, Bulletin de la Societe Chimique de France, 11–12 (1982) I-427.
[23] K. Inamura, R. Iwamoto, A. Iino, T. Takyu, J. Catal. 142 (1993) 274.

[24] P.J. Mangnus, A. Riezebos, A.D. van Langeveld, J.A. Moulijn, J. Catal. 151 (1995) 178.

[25] P. Arnoldy, Ph.D. Thesis, University of Amsterdam, Netherlands, 1985.

[26] C.D. Wagner, L.E. Davis, M.V. Zeller, J.A. Taylor, R.M. Raymond, L.H. Gale, Surf. Interface Anal. 3 (1981) 211.

[27] U. Lindner, H. Papp, Appl. Surf. Sci. 32 (1988) 75.

[28] E. Paparazzo, Appl. Surf. Sci. 25 (1986).

[29] C.F. Jones, S. LeCount, R.C. St, T.J. White, Appl. Surf. Sci. 55 (1992) 65.

[30] J.J. Phillipson, in: Catalyst Handbook, Wolfe Scientific Books, 1970, p. 46.

[31] C.K. Groot, A.M. Van der Kraan, V.H.J. de Beer, R. Prins, Bull. Soc. Chim. Belg. 93(8)(9) (1984) 707.

[32] D. Briggs, M.P. Seah, in: Practical Surface Analysis, 2nd ed., vol. 1, Wiley, Chichester, 1990.

[33] K. Laajalehto, I. Kartio, P. Nowak, Appl. Surf. Sci. 81 (1994) 11.